Transactions of the Korean Nuclear Society Virtual Spring Meeting
July 9-10, 2020

Validation of LHF Experiment Using MELCOR and ANSYS Mechanical

Yeon Soo Kim, Kukhee Lim*, Yong Jin Cho
Korea Institute of Nuclear Safety 62 Gwahak ro, Yuseong-gu, Daejeon 305-338, Republic of Korea
**Corresponding author: limkh@kins.re.kr*

1. Introduction

If core materials are relocated to a reactor lower plenum during severe accidents, the lower head can be exposed to thermal and mechanical loads. The global failure of lower head may occur due to creep rupture, which is type of failure by high creep strain. Creep is a time-dependent deformation under the constant mechanical stress. Deformation of the lower head during severe accident may be caused mainly by creep because of relocated high-temperature core materials and high in-vessel pressure of a reactor.

Prediction of timing, size and location of failure is important because they are the initial condition of severe accident involving ex-vessel phenomena such as direct containment heating, molten corium-concrete interaction and fuel coolant interactions [1].

Severe accident analysis codes like MAAP [2] and MELCOR [3] predict the timing and location of failure with the damage based on the life-fractional rule. The damage is calculated from Larson-Miller parameter as a function of stress and temperature. MELCOR has two options to calculate the stress; zero-dimensional and one-dimensional models. The models in these codes originally have been developed to predict the global creep failure of LHF and OLHF experiments [4].

However, their applicability has not been validated appropriately. In this study, several LHF experiments are analyzed to validate the lower head failure models of MELCOR.

2. Modeling

2.1 Validation matrix from LHF experiments

The objective of LHF experiments was to characterize the failure mode, timing and size of lower head under various severe accident conditions. The test matrix of the LHF experiments is shown in Table I.

Table I: Summary of LHF experiments

Test	Heat Flux Distribution	Structure Elements	Pressure	Heater
LHF-1	Uniform	-	10 MPa	Resistance
LHF-2	**Center-peaked**	**-**	**10 MPa**	**Resistance**
LHF-3	Edge-peaked	-	10 MPa	Resistance
LHF-4	Uniform	Penetrations	10 MPa	Resistance
LHF-5	**Edge-peaked**	**Penetrations**	**10 MPa with Transient**	**Induction**
LHF-6	Uniform	Weldment	10 MPa	Induction
LHF-7	Uniform	-	5 MPa	Induction
LHF-8	Edge-peaked	-	10 MPa	Induction

* Items in bold are not included in this validation.

The effect of heat flux distribution was confirmed through the first three experiments; uniform, center-peaked and edge-peaked. LHF-1 is the reference test with uniform heat flux in order to simulate massive relocation of core materials on the lower head. LHF-2 is to simulate the TMI-2 like thermal loading with center-peaked heat flux. The edge-peaked heat flux in LHF-3 is to simulate focusing effect with two-layered molten pool configuration. The effect of penetrations and weldment on failure time was examined through LHF-4, 5 and 6. In case of LHF-5, an unplanned pressure transient occurred so that those effect was additionally investigated. The pressure effect was identified through LHF-7 experiment. LHF-8 is similar with LHF-3 except the heating method.

Some experiments are excluded from the validation. Firstly, LHF-2 is not appropriate for validation since the deformation is concentrated only to the heated area. As MELCOR calculates the hoop stress with the radius of the lower head, the stress cannot be evaluated using MELCOR. Secondly, thermal loading of LHF-5 is not axisymmetric owing to the unexpected test environment. This unusual temperature distribution cannot be simulated using MELCOR which assumes symmetric thermal and mechanical loading conditions.

2.2 MELCOR input deck

Input decks for both MELCOR 1.8.6 and 2.2.14959 are prepared in this study. Input decks of LHF experiments have been initially developed by IBRAE using MELCOR 1.8.6. They are converted to MELCOR 2.2.14959 by using the SNAP interface. Fig. 1 describes control volume nodalization of MELCOR input for LHF test vessel. The lower plenum is composed with 9 of total 14 control volumes. The height of each volume reflects the location of 9 thermocouples

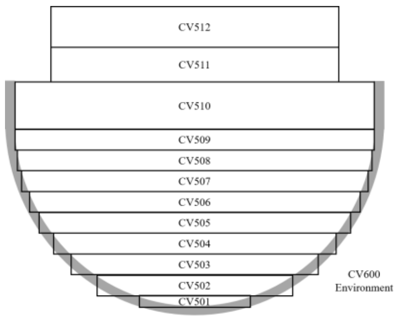

Fig. 1. Control volume nodalization of MELCOR for LHF test vessel

The temperature boundary conditions of the in-vessel wall are applied to each segment of the lower head using the CF package of MELCOR. Fig. 2 shows the segment numbers starting with 1 from the below. The input temperature and pressure conditions are verified by comparing the experimental data with various azimuthal angle for all tests in validation matrix. Fig. 3 to 5 and 6 compares the temperature and pressure applied to LHF-1, respectively.

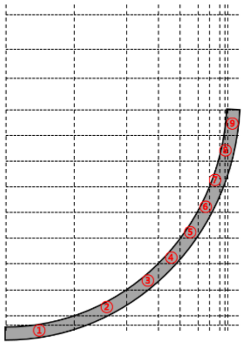

Fig. 2. Cell nodalization of MELCOR for LHF test vessel

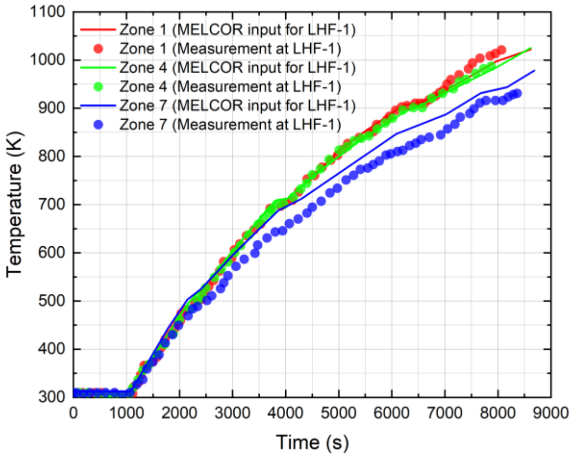

Fig. 3. Comparison of MELCOR 2.2.14959 input function and measurement of temperature at zone 1, 4 and 7 in LHF-1

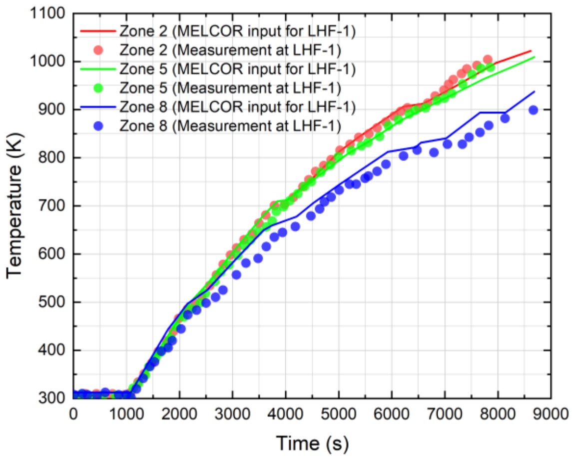

Fig. 4. Comparison of MELCOR 2.2.14959 input function and measurement of temperature at zone 2, 5 and 8 in LHF-1

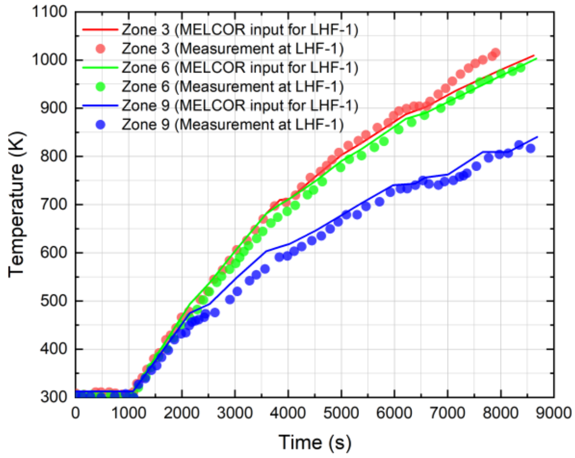

Fig. 5. Comparison of MELCOR 2.2.14959 input function and measurement of temperature at zone 3, 6 and 9 in LHF-1

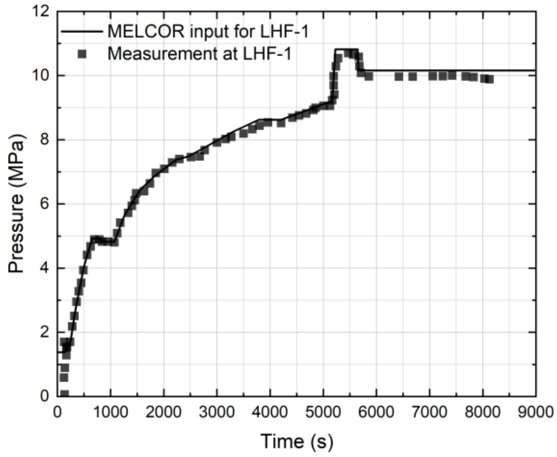

Fig. 6. Comparison of MELCOR 2.2.14959 input function and measurement of pressure at LHF-1

2.3 Review of MELCOR models

There are two failure modes of lower head in MELCOR; creep rupture and thru-wall yielding. Creep rupture is predicted based on life-fractional rule as shown in Eq. (1). When the accumulated damage becomes 1, the lower head fails by creep rupture. Rupture time t_R is defined in Eq. (2) with Larson-Miller parameter P_{LM}. P_{LM} in Eq. (3) is a function of effective stress σ_e.

$$\sum \frac{\Delta t}{t_R} = 1 \quad (1)$$

$$t_R = 10^{\left(\frac{P_{LM}}{T} - 7.042\right)} \quad (2)$$

$$P_{LM} = 4.812 \times 10^4 - 4.725 \times 10^3 \log \sigma_e \quad (3)$$

MELCOR provides two options for the stress calculation; 0-and 1-dimensional model. 0-dimensional model adopts hoop stress which is constant through the thickness of a segment as shown in Eq. (4). Meanwhile, 1-dimensional model calculates the stress distribution through the layer. The stress as a function of thickness is implicitly calculated using the Eq. (5) ~ (7).

$$\sigma_e = \frac{(\Delta P + \rho_d g \Delta z_d) R_i^2}{R_o^2 - R_i^2} \tag{4}$$

$$(\Delta P + \rho_d g \Delta z_d) R_o^2 = \sum_i^{N_{NY}} \sigma_i (R_i^2 - R_{i-1}^2) + \sum_j^{N_Y} \sigma_Y(T_j)\left(R_j^2 - R_{j-1}^2\right) \tag{5}$$

$$\sigma_i = E(T_i)[\varepsilon_{tot} - (\varepsilon_{pl,i} + \varepsilon_{th,i})] \tag{6}$$

$$\varepsilon_{pl,i}(t + \Delta t) = \varepsilon_{pl,i}(t) + 0.18 \frac{\Delta t}{t_R} \tag{7}$$

On the other hand, thru-wall yielding is predicted when the stress in all layer consisting of the segment becomes larger than the yield strength. Thru-wall yielding is the failure mode predicted only by 1-dimensional model.

3. Results and Discussion

3.1 Creep rupture

Table II and III show the failure timing by different code versions and MELCOR stress models. Little difference is observed according to the code version. The failure mode is ‘creep rupture’ for all cases. The failure timing by 1-dimensional model is slightly earlier than 0-dimensional model. It is because the stress at the in-vessel wall by 1-dimensional model is higher than 0-dimensional model as shown in Fig. 7. The higher stress results in shorter rupture time.

On the other hand, the timing predicted by both 0 and 1-dimensional model in MELCOR was delayed than the observation due to the underestimated stress. In general, as the wall is getting thinner due to deformation by creep, the stress gets larger accordingly. Since Mechanical considers the wall thinning effect, the stress gets larger rapidly as shown in Fig.8 so that the failure timing was reasonably predicted. However, as MELCOR does not consider the geometrical deformation, the stress is determined mainly by the internal pressure at the specified radius. The small stress causes the underestimation of accumulative damage so that the failure time is delayed.

In case of LHF-4, the large deviation between prediction and observation was obtained about 23,500 s. The temperature and pressure in LHF-4 was entered only until 15,000 s. After the time, the temperature and pressure was calculated with the value at 15,000 s. Therefore, it can be concluded that MELCOR nearly fails to predict the failure of LHF-4.

Table II: Comparison of failure timing, mode and location predicted by MELCOR 1.8.6 and measured in LHF experiments

Test	0-dimensional model	1-dimensional model	Experiment
LHF-1	12,214 s (Creep rupture at 1)	12,009 s (Creep rupture at 1)	8,700 s (Creep rupture at 1)
LHF-3	15,589 s (Creep rupture at 6)	15,255 s (Creep rupture at 6)	10,680 s (Creep rupture at 5)
LHF-4	40,801 s (Creep rupture at 3)	39,703 s (Creep rupture at 3)	16,200 s (Weld failure at 1)
LHF-6	15,389 s (Creep rupture at 1)	15,159 s (Creep rupture at 1)	11,280 s (Creep rupture at 1)
LHF-7	19,853 s (Creep rupture at 1)	19,692 s (Creep rupture at 1)	18,400 s (Creep rupture at 1)
LHF-8	22,405 s (Creep rupture at 5)	22,101 s (Creep rupture at 5)	14,820 s (Creep rupture at 7)

Table III: Comparison of failure timing, mode and location predicted by MELCOR 2.2.14959 and measured in LHF experiments

Test	0-dimensional model	1-dimensional model	Experiment
LHF-1	12,211 s (Creep rupture at 1)	12,006 s (Creep rupture at 1)	8,700 s (Creep rupture at 1)
LHF-3	15,588 s (Creep rupture at 6)	15,254 s (Creep rupture at 6)	10,680 s (Creep rupture at 5)
LHF-4	40,806 s (Creep rupture at 3)	39,707 s (Creep rupture at 3)	16,200 s (Weld failure at 1)
LHF-6	15,386 s (Creep rupture at 1)	15,156 s (Creep rupture at 1)	11,280 s (Creep rupture at 1)
LHF-7	19,854 s (Creep rupture at 1)	19,693 s (Creep rupture at 1)	18,400 s (Creep rupture at 1)
LHF-8	22,407 s (Creep rupture at 5)	22,103 s (Creep rupture at 5)	14,820 s (Creep rupture at 7)

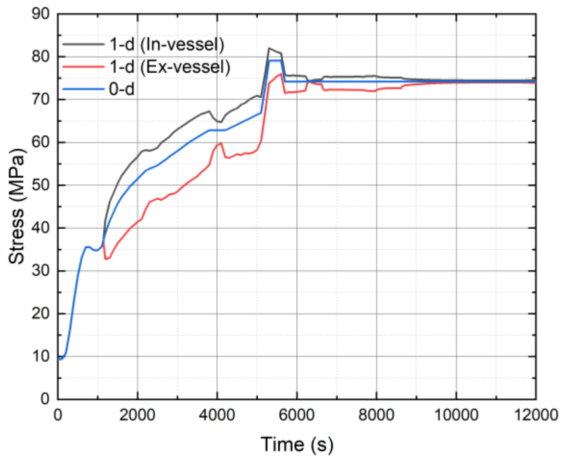

Fig. 7. The stress of each node at segment 1 in LHF-1 experiment calculated by MELCOR 2.2.14959

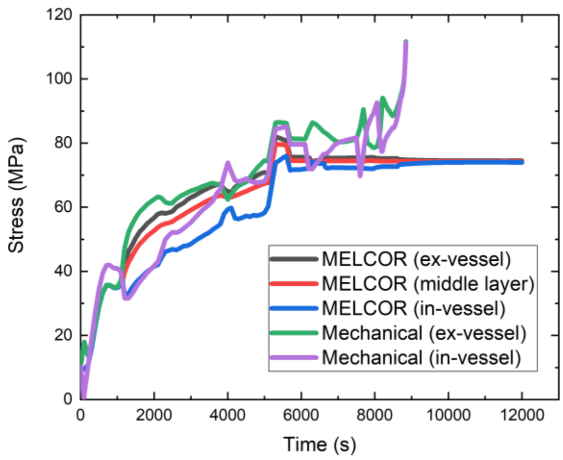

Fig. 8. The stress of each node at segment 1 in LHF-1 experiment calculated by MELCOR 2.2 and ANSYS Mechanical

3.2 Thru-wall yielding

Yield strength σ_Y is also required in 1-dimensional model to calculate the equivalent stress σ_i. However, the MELCOR default correlation for yield strength is different from the measurement in OLHF experiment as described in the Fig. 9. Thus, for more exact failure prediction, the yield strength was modified into the OLHF data in this section. Table IV shows the comparison of failure timing, mode and location estimated by 1-dimensional model in MELCOR 2.2.14959 with yield strength of MELCOR default and OLHF data.

Failure by thru-wall yielding is predicted at LHF-1, 6 and 7 when yield strength of OLHF data is used. The failure timing by thru-wall yielding is much earlier than that by creep rupture using the MELCOR default yield strength. Because the yielding strength of OLHF data at high temperature region is lower than that of MELCOR default, the effective stress by Eq. (6) approaches to σ_Y earlier. Fig. 10 compares the equivalent stress by 1-dimensional model and the yield strength at each temperature node. As shown in Fig. 10, every yield strength decreases gradually and becomes equal to the effective stress about 8,600 s. Then failure occurred.

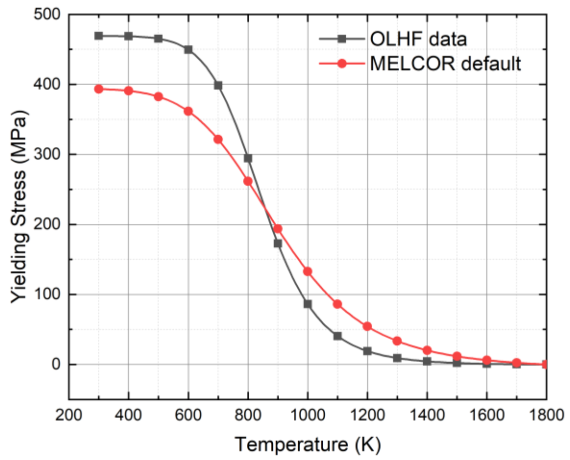

Fig. 9. Yield strength calculation for OLHF data and MELCOR default

Table IV: Comparison of failure timing, mode and location predicted by 1-dimensional model in MELCOR 2.2.14959 with OLHF data and MELCOR default and measurement

Test	MELCOR default	OLHF data	Experiment
LHF-1	12,006 s (Creep rupture at **Seg. #1**)	8,694 s (Thru-wall yielding at 4)	8,700 s (Creep rupture at 1)
LHF-6	15,156 s (Creep rupture at 1)	11,480 s (Thru-wall yielding at 2)	11,280 s (Creep rupture at 1)
LHF-7	19,693 s (Creep rupture at 1)	16,462 s (Thru-wall yielding at 1)	18,400 s (Creep rupture at 1)

* Items in bold is the segment number of the lower head shown in Fig. 2.

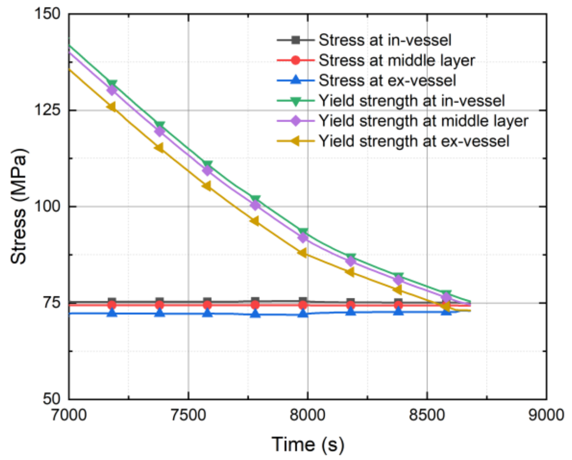

Fig. 10. comparison of yield strength of OLHF correlation and effective stress through the segment 1 at LHF-1.

4. Conclusion

In this study, the MELCOR models for lower head failure prediction was reviewed and validated by comparing with the result of LHF experiments. As a result, the failure time of all the cases simulated with default yield strength was later than the time observed in LHF experiment. The delayed time was caused by the stress calculation which does not consider the wall-thinning effect. For the cases simulated with the yield strength based on OLHF data, the lower head failed by thru-wall yielding in LHF-1, 6 and 7 at the earlier timing. These results showed that the accuracy of failure timing, mode and location predicted by MELCOR models are unsatisfactory. In the future work, the finite element model (FEM) analysis will be conducted to derive the limit of MELCOR models more quantitatively.

REFERENCES

[1] CHU, T. Y., et al. Lower Head Failure Experiments and Analysis. Report, NUREG/CR-5582, SAND98-2047, Sandia National Laboratories, Albuqerque, NM, 1999.

[2] FAI, User's Manual for MAAP4: modular accident analysis program for LWR power plants. Illinois. United States of America: Fauske and Associates, LLC; 1994.

[3] Humphries L. L. et al., "MELCOR Computer Code Manuals, Vol. 2: Reference Manual, Version 2.1.6840," SAND 2015-6692R, Sandia National Laboratories, August 2015.

[4] HUMPHRIES, L. L., et al. OECD Lower Head Failure project Final report. Sandia National Laboratories, Albuquerque, NM, 2002, 87185-1139.